Hindawi
Shock and Vibration
Volume 2019, Article ID 1873479, 13 pages
https://doi.org/10.1155/2019/1873479

Research Article

Construction Process Simulation and In Situ Monitoring of Dendritic Structure on Nanjing Niushou Mountain

Wenying Zhang,[1] Shaole Yu ,[2] Xuewei Zhang,[2] Junsheng Yan,[2] and Xinxi Chen[2]

[1]*College of Civil Engineering, Beijing University of Technology, Beijing 100124, China*
[2]*China Construction Eighth Engineering Division Co., Ltd., Shanghai 200135, China*

Correspondence should be addressed to Shaole Yu; yushaole10@163.com

Received 29 March 2019; Revised 16 June 2019; Accepted 9 July 2019; Published 28 July 2019

Academic Editor: Luca Landi

For complex structures, where there are great differences between the structural form in the construction process and the design forming state, mechanical analysis of the construction process is required. The dendritic structure on Nanjing Niushou Mountain is taken as an engineering case study, with a narrow construction space, weak construction platform, and difficulty in setting the equipment in the site. A new construction method, self-balancing elevating scheme, is introduced according to the special condition of the construction field. The lifting frame and the connection joint between the trunk and the branch employed in the self-balancing elevating scheme are optimized according to the structure's behavior. A construction monitoring scheme was adopted in this project to ensure construction safety. The maximum cable force and deformation occurred at the beginning of the lifting. The construction process simulation was conducted by space structure design software 3D3S. The analysis results were well consistent with the in situ construction monitoring results. The analysis results show that the self-balancing elevating scheme could satisfy the construction requirement on the special construction condition and provide reference on future practical application.

1. Introduction

Bionic structure is imitating biological stress principles to design buildings. Dendritic form is common in nature, and dendritic structure was first put forward as a structure concept by German architect Otto in the 1960s. Dendritic structure, with its unique form and elegant appearance, had been gradually applied in buildings all over the world. Famous global engineering applications including Germany's Stuttgart airport terminals, East Station in Lisbon, Portugal, and Shenzhen Cultural Center and Changsha South Railway Station in China are shown in Figure 1. For those complex steel structures, it is very important to choose reasonable construction scheme. Xiao [1] described the history of integral lifting technology, and some typical engineering applications were shown. In the early 1970s, the integral lifting technology was used in the construction of the large-scale stadium's network in Osaka large-scale comprehensive stadium. The lifting height reached 52.46 m, and the lifting weight reached more than 4700 t. According to the research findings from Hou et al. [2], the integral hoisting method was adopted in Singapore MEGA Meeting and Exhibition Center, which was a large-span steel structure with a total weight of 8000 t, and a maximum height of 22 m. Li et al. [3] introduced the construction process of Beijing Olympic Water Cube Water Project; the main stadium of Beijing Olympic Water Cube Water Project, with lifting weight of 6300 t and lifting height of 30 m, was constructed by bulk-way assembly technology at high altitude. Lu et al. [4] introduced the construction process of T3 terminal building of Chongqing Jiangbei International Airport; the high-altitude slip method was adopted in the steel structure engineering of the main building of T3 terminal building, which was a space curved surface with lifting height of 49 m and lifting weight of 6000 t. The advantage of integral lifting method is that there is no need to build temporary brackets, and the amount of work at high altitude is small. The structural components

(a) (b) (c) (d)

Figure 1: Application of dendritic structure in domestic and foreign projects. (a) Stuttgart airport terminals, Germany. (b) East Station in Lisbon. (c) Shenzhen Cultural Center. (d) Changsha South Railway Station.

can be assembled on the ground, and the welding quality can be ensured. The disadvantage of the overall lifting method is that the control of synchronous lifting is difficult and the construction risk coefficient is high. The construction method of integral hoisting method requires high construction machinery. The tonnage requirement of crane usually reaches 100 t, 300 t, or even 600 t, and this has a relatively high requirement for the bearing capacity of the crane's location. The bulk-way assembly technology at high altitude needs a lot of scaffolding materials to build support frame. The construction difficulty of high-altitude sliding method lies in the laying of sliding track, which requires effective control of the rigidity, deformation, and stability of sliding track. In this paper, the dendritic structure on Nanjing Niushou Mountain is taken as an engineering case study with narrow construction space, weak construction platform, and difficulty in setting the equipment in the site. A new construction method, self-balancing elevating scheme, was introduced according to the field conditions. The self-balancing elevating scheme is composed of lifting frame, cable, and hydraulic lifting device. The cables (called active cables) on one side of the lifting frame are connected to the structure to be elevated, and the cables on the other side are used to balance the tension in the active cables; the hydraulic lifting device is employed to lift the structure to the design position. Compared with the methods described above, the self-balancing elevating scheme does not need to build temporary brackets, and the amount of work at high altitude is small. Moreover, the structural components can be assembled on the ground, and the welding quality can be ensured. However, the mechanical properties in the construction process and the final state of completion are quite different. Therefore, mechanical analysis of the construction process is required for the complex structures. At the end of the 19th century, Meshchersky [5] first proposed time-varying rigid body mechanics. Southwell [6] studied the time-varying mechanism of a thick-walled cylinder that wraps a wire around an elastic shaft. From the late 1980s to the 1990s, scholars in many countries have carried out studies on the basic concepts and basic theories of time-varying mechanical systems. Naumov [7] summarized these findings in his research. In China, Cao [8] also conducted systematic research on some basic theories of time-varying mechanics, gradually forming the framework of a time-varying mechanical system. The numerical methods for the analysis of construction mechanics problems include the finite element method, the time-varying element method, the topological change method, and some other analysis methods. The most widely used method is the finite element method. Construction monitoring is an important guarantee for construction safety and structural construction according to the research findings from Li and Ou [9]. For those complex structures, structural monitoring systems are an important safety guarantee for structural construction, which have been extensively employed in civil structures. The variation regularity of vibration, deflection, and strain responses of 522 m Foyle Bridge girders have been launched through various sensors by Housner et al. [10]. Sloan et al. [11] investigated the structural dynamic responses and

deformations of the 12.9 km Confederation Bridge through an integrated monitoring system. Li et al. [12] conducted the monitoring of the wind-induced response characteristics of a 63-story reinforced concrete tall building under strong wind conditions through full-scale measurements. Su et al. [13] monitored the structural performance of the Shanghai Tower during its construction and service stages through a monitoring system that consists of more than 400 sensors. In this paper, the dendritic structure on Nanjing Niushou Mountain is taken as an engineering case study with narrow construction space, weak construction platform, and difficulty in setting the equipment in the site. A new construction method, self-balancing elevating scheme, was introduced according to the field conditions. The construction process simulation was conducted by finite element software, and the whole construction process was monitored during construction. The distribution pattern of the stress and deformation of structure during the construction process were analyzed, and the safety of the construction process was examined.

2. Engineering Situation

The palace roof structure was the first phase project of the cultural tourist attraction of Nanjing Niushou Mountain, located at Nanjing, China. The building area was 20,000 square meters, and the overall effect is shown in Figure 2. The roof was single-layer reticulated shell structure in the form of an irregular surface, which is the biggest single layer in China and Asia. Its largest span was 130.0 meters, and the height was 56.3 meters. The western side of the roof along the outer edges was supported on the lower slopes, and the middle and the east were all open. The roof structure system was only supported by four dendritic steel columns set in axis 11-1, 11-2, 11-3, 11-4 (2 big dendritic steel structure columns and 2 small dendritic steel structure columns). Dendritic support structure set in axis 11-2 and axis 11-3 was the main emphasis and main difficulty of the construction in this project. In order to distinguish between columns, they were called the north big tree and the south big tree in the paper. The trees both included 1 trunk and 12 branches. Each branch was divided into 2 small branches in certain elevations. The tallest point of big tree was 50.956 meters. In order to adapt to architectural appearance, each support structure was made up of 12 octagon variable cross-sectional steel structure columns. The 7-A branch of the south big tree had a maximum weight of 71.14 tons with a length of 52.66 meters. The 13-C branch of the north big tree had a minimum weight of 15.47 tons. The weight details of all branches are shown in Figure 3.

3. Construction Scheme

The north tree and the south tree were 1,000 tons in total. The single heaviest branch reached 70 tons. As a large steel structure project, the construction technique of large steel structures commonly used for installing, which has been investigated by Cui et al. [14] and Lin et al. [15], was collected before determining the installation scheme. They could be mainly divided into 7 types as follows: high altitude construction in bulk, sliding construction, member assembly, whole installation, integral lifting, integral propping up, and folding expansion. Because of the elliptical concrete structure built under the roof on the east side and the west mountain, the dendritic structure construction platform could only be completed on the basement roof, which only allows no more than a 75 t crane. Large machinery and equipment could not enter the site. Due to the dendritic column installation site and space being narrow, the construction period was short. Therefore, conventional techniques for installation were not suitable for this project. Combined with site condition and the progress requirements, a new construction scheme, self-balancing elevating scheme, was introduced to complete the installation of the branches.

3.1. Self-Balancing Elevating Construction Scheme. Self-balancing elevating construction scheme meant synchronously or asynchronously lifting a pair or more branches and setting a certain number of cables to balance force generated in the lifting process, which could make the whole system in balance. For this project, as the branches have a big difference in weight, elevating schemes with asynchronously lifting were adopted. As shown in Figure 4, the construction team firstly used small devices to lift three small branches, corresponding to the big branches which would be subsequently elevated to design position. Each small branch was linked to the lifting frame and trunk bottom, respectively, through two cables. They then assembled the big branches horizontally and linked them to the hydraulic lifting device through system. Then, the construction team gradually lifted the big branches to design position through a hydraulic lifting device located on the top of the lifting frame. As shown in Figure 5, the active cable force F_a decreases with the increase of branch height; therefore, the active cable force F_a is the greatest at the moment of initial position. The horizontal components of the active cable force F_{ah} were balanced by the horizontal forces of cables; the relationship is shown in formula (1). F_{1h}, F_{2h}, and F_{3h} indicate the horizontal forces of cable No. 1, No. 2, and No. 3, respectively. α_1, α_2, and α_3 represent the angle between the horizontal projection of cable No. 1, No. 2, and No. 3 and the horizontal projection of active cable, respectively:

$$F_{ah} = F_{1h}\cos\alpha_1 + F_{2h}\cos\alpha_2 + F_{3h}\cos\alpha_3. \quad (1)$$

3.2. Lifting Frame Design. In the process of lifting, the lifting frame plays an important role. The lifting frame, branches, and cables form a whole structure system. Therefore, the design of the lifting frame was very important. The lifting tower was four tube lattice columns. The chord and strip were both steel tubes. The lifting frame was 24 m tall, 2 m long, and 2 m wide. Each section was 2 m tall, and there were 12 sections in total. The

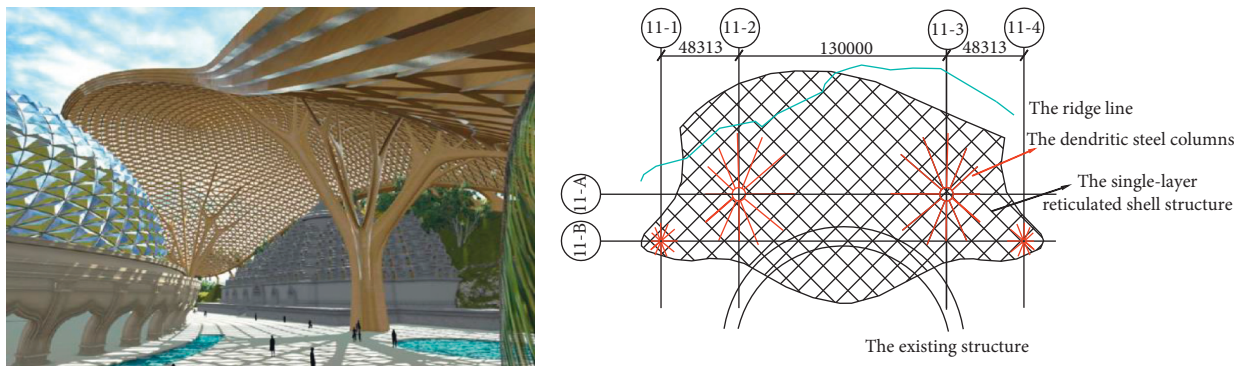

Figure 2: Schematic diagram of dendritic structure on Niushou Mountain. (a) Design sketch. (b) Plan view.

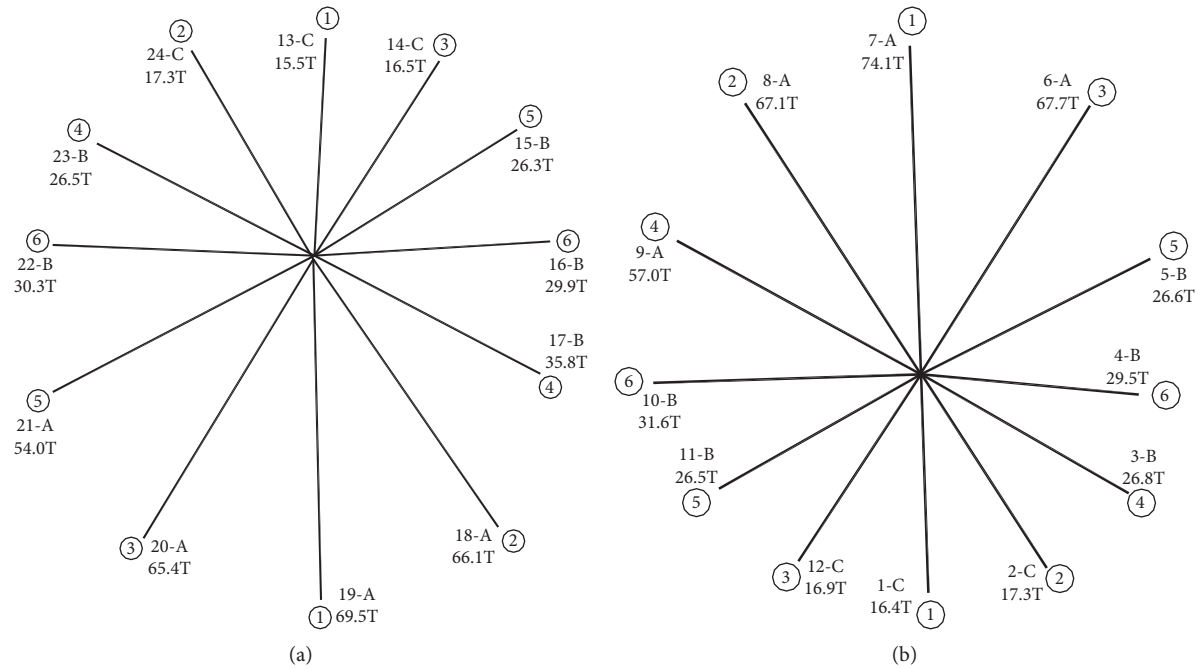

Figure 3: Weight chat of dendritic structure. (a) North tree. (b) South tree.

original lifting frame scheme model is shown in Figure 6(a). Due to the horizontal component, the force of the cable could not be balanced at the starting state, which will make the lifting frame suffer compression bending. Integral analysis showed that the stress ratio of the chord on one side of the lifting frame was too large, so the tower was adjusted to spindle lattice masts, which is shown in Figure 6(b). Because the spindle lattice masts were hinged on both ends, the lifting frame changed from compression-bending member to axial compression member. The maximum stress ratio of the lifting chord decreased from 0.98 to 0.657, a reduction of 33%. The finite element model of the lifting frame was established in ANSYS, and the stability analysis of the lifting frame was carried out. Beam188 element was adopted to simulate the lifting frame, and each member was divided into 10 beam elements. The constitutive model was simulated by bilinear follow-up strengthening model BKIN. The buckling analysis of the lifting frame was conducted, and the vertical load applied at the top is taken as the sum of the vertical components of each cable force. The primary four buckling modes are shown in Figure 7; the first buckling mode is X-direction bending buckling, the second buckling mode is Y-direction bending buckling, the buckling coefficient is 57.646, and the buckling load is 99151.12 kN. The third and fourth buckling modes are local buckling with buckling coefficients of 78.762 and 78.764. According to the results of buckling analysis, the first mode is taken as defect distribution. The elastic-plasticity finite element analysis of the model was conducted, as shown in Figure 8. It can be concluded that the structure is in an elastic state before loading to 3.4 times load, and the structure reaches the ultimate bearing capacity when loaded to 4.1 times load.

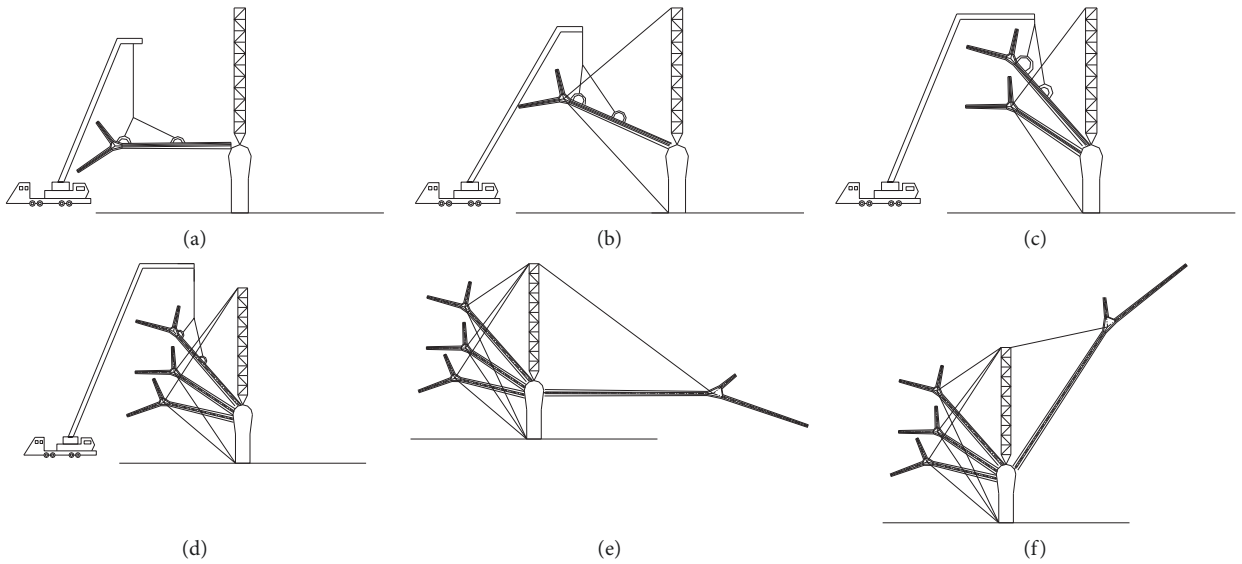

Figure 4: Self-balancing elevating scheme. (a) lifting the first small branch; (b) lifting the first small branch to design position and anchoring cables; (c) installing the second small branch; (d) installing the third small branch; (e) assembling the big branch horizontally; (f) lifting the big branch to design position.

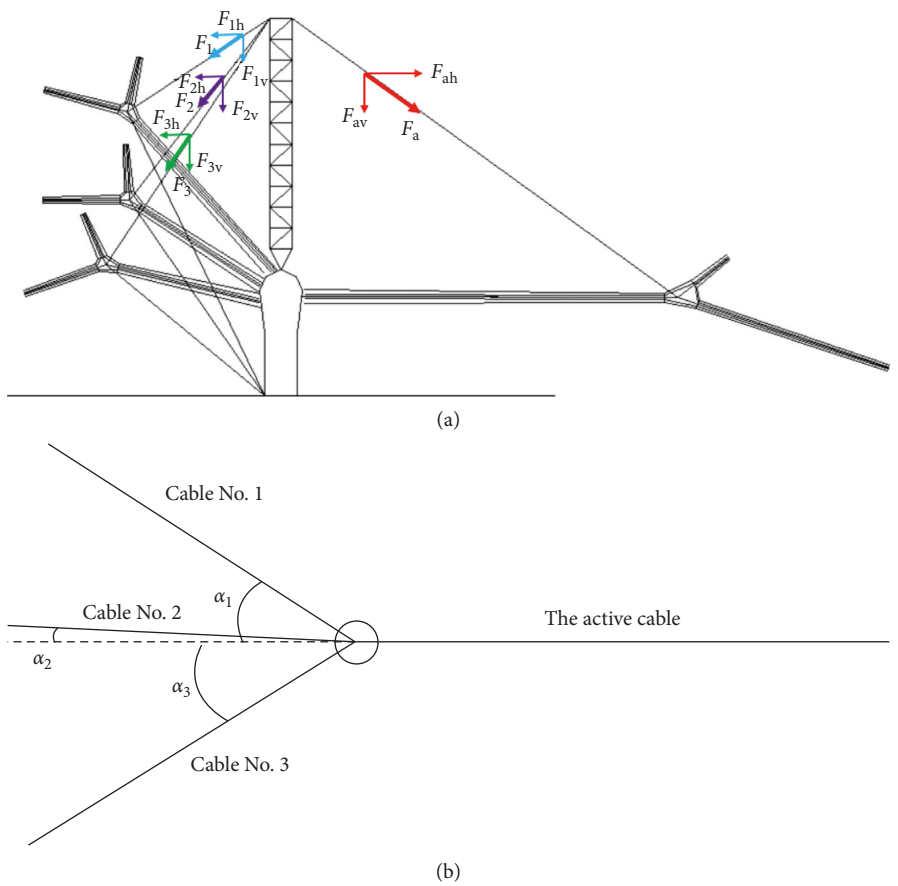

Figure 5: Force diagram of cable. (a) Diagram of cable force. (b) Plane projection diagram of cable.

3.3. Joint Design of Trunk and Branches. The design of the connection joint between the trunk and the branch has a greater impact on the construction progress. The original connection joint scheme is designed to achieve the effect of the shaft by welding the ear plate on the outside of the section and inserting the pin, as shown in Figure 9. However, there are several shortcomings in this program. Insufficient stiffness of the joint may lead to excessive

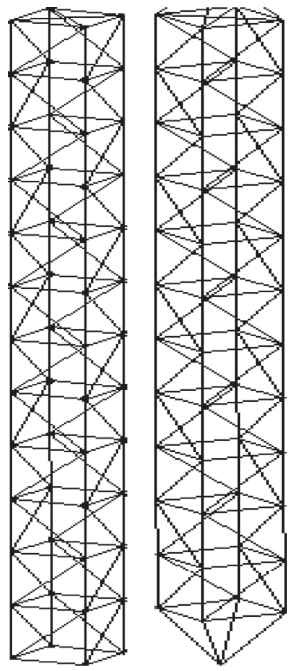

Figure 6: Construction scheme of lifting frame. (a) Original scheme. (b) New scheme.

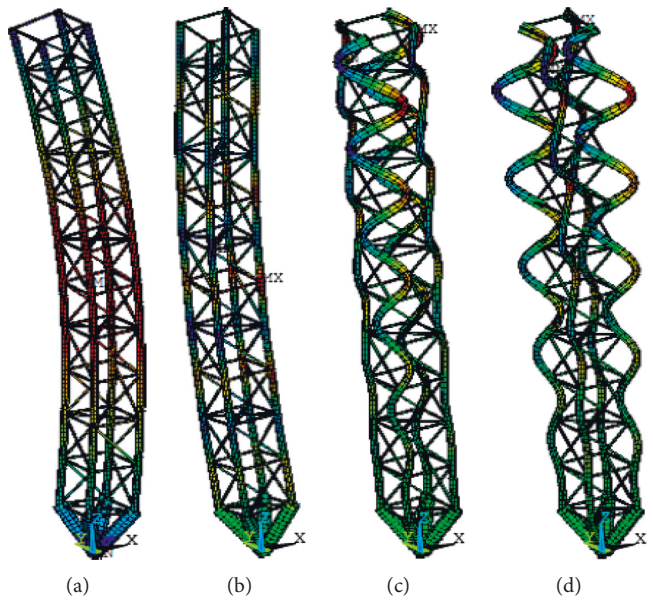

Figure 7: First four buckling modes. (a) First buckling mode. (b) Second buckling mode. (c) Third buckling mode. (d) Fourth buckling mode.

deformation and connection damage, and the ear plate and pin cross sections are too small to cause the connection strength failure. In order to ensure the safety of the lifting process and speed up the construction progress, a new connection joint scheme was proposed, as shown in Figure 10. The branches and trunks were connected by the pin joint. In order to improve the strength of the joint, a round steel plate with a diameter of 400 mm and a thickness of 30 mm was set on each side of the ear plate. The materials for the connection joint and the round steel plate were both Q345. The steel presented yield strength of 345 MPa and elasticity modulus of 210 GPa.

Through calculation and analysis, the pin suffered a standard maximum axial load of 1233.06 kN in the construction process and an in-plane standard vertical load of 213.07 kN. The force conditions of the pin joint were divided into three stages, which are shown in Table 1. When analyzing the out-of-plane disturbance influence in

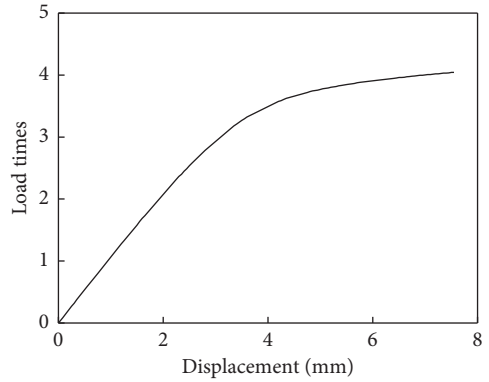

Figure 8: The load times-displacement curve.

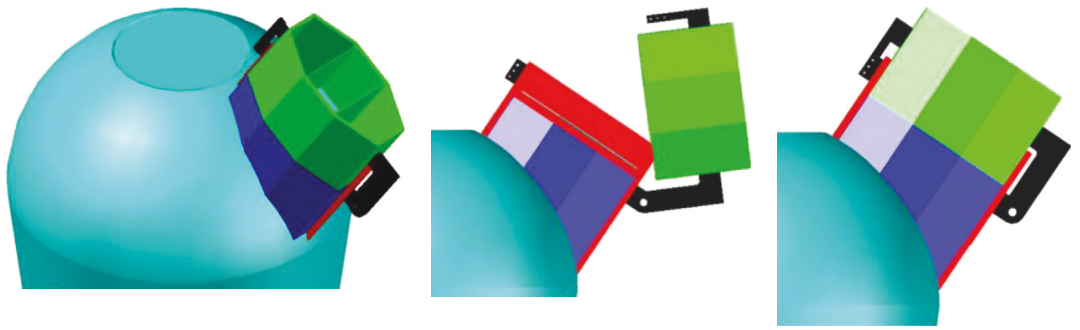

(a) (b) (c)

Figure 9: The original scheme of connection. (a) 3D schematic. (b) Initial state of the connection. (c) Completion status of the connection.

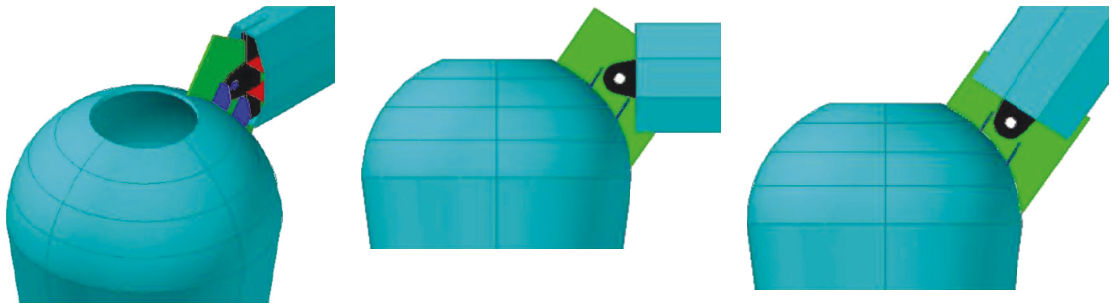

(a) (b) (c)

Figure 10: The new scheme of connection. (a) 3D schematic. (b) Initial state of the connection. (c) Completion status of the connection.

Table 1: Division of construction stages.

Stage	Name	Reason
1	Hoisting emplacement	In this stage, the pin joint was subjected to vertical shear force generated by gravity.
2	Lower cable fixation	In this stage, the pin joint was subjected to horizontal shear force generated by horizontal components of active cable.
3	Out-of-plane disturbance	In the process of lifting, there might be out-of-plane disturbance. The pin joint was subjected to horizontal shear force generated by horizontal components of active cable; at the same time, the joints were subjected to out-of-plane loads due to out-of-plane disturbances.

the lifting process, the axial force dynamic effect was calculated by 2 times the standard value of the maximum axial load of the pin joint, and the 10% of axial force was taken as the external force of the surface. The solid model of the gusset plate was established by using ABAQUS. As shown in Figure 11, in the hoisting emplacement stage,

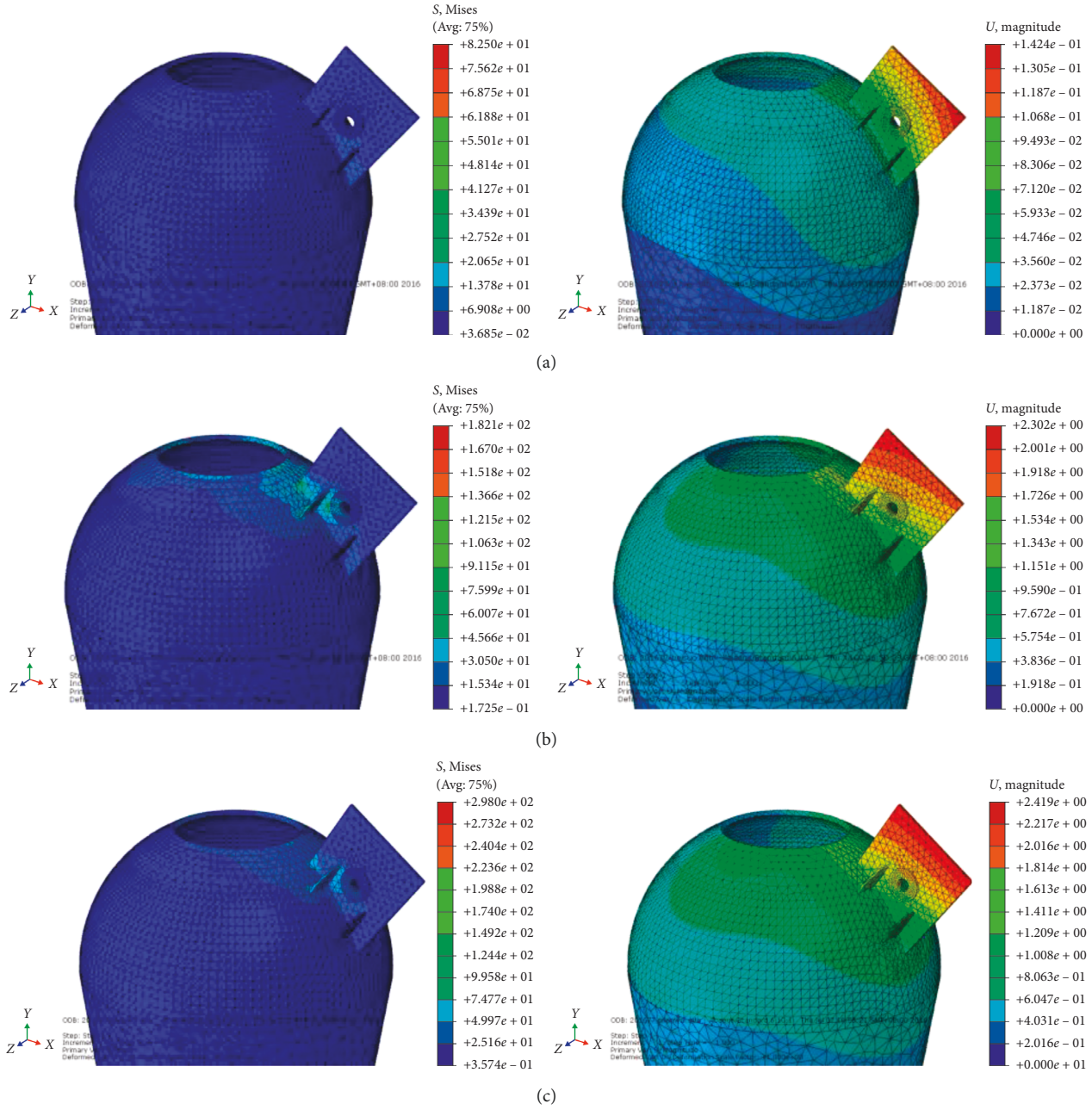

Figure 11: Stress and deformation nephograms under three different construction stages. (a) Stress and deformation nephograms in the hoisting emplacement stage. (b) Stress and deformation nephograms in lower cable fixation stage. (c) Stress and deformation nephograms in out-of-plane disturbance stage.

the maximum stress was 82.5 MPa and the maximum deformation was 0.142 mm. In the lower cable fixation stage, the maximum stress was 182.1 MPa and the maximum deformation was 2.302 mm. In the out-of-plane disturbance stage, the maximum stress was 298 MPa and the maximum deformation was 2.419 mm, which meets the construction requirements. In order to avoid the adverse effects of the out-of-plane disturbance on the root pin and ensure construction safety, double-supported frames are used to prevent out-of-plane movement. A track gap for the big branch lifting was formed by using two supported frames, and the two supported frames were connected with steel beams at a certain height to keep stability.

4. Monitoring Scheme

To ensure construction safety, a construction monitoring scheme was adopted in this project. Taking the heaviest No. 7 branch as an example, the cable and joint were labelled, as shown in Figure 12. The cable connecting the big branch and the lifting frame is called the active cable, the cable connecting the small branch and the lifting frame is called the upper cable, and the cable connecting the

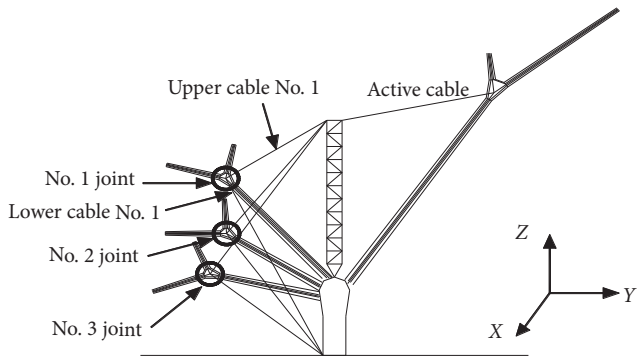

Figure 12: Cable label.

small branch and trunk bottom is called the lower cable. In order to distinguish the cable between the three branches, the joint number was added in the cable label. The reflectors were arranged on the No. 2 joints and the top of the lifting tower, and the deformation monitoring of the key positions in the lifting process was carried out by the total station. The real-time data of cable force of the active cable and the upper cable No. 2 were read by the lifting equipment.

The cables were made up of 12 steel strands, whose diameter was 17.8 mm and strength was 1860 MPa. Three samples of steel strands were taken to conduct mechanical property tests. The results are shown in Table 2.

5. Construction Process Simulation

The 3D3S spatial analysis software was used to establish the model of the whole dendritic structure. In order to compare numerical simulation results and the construction monitoring data, the construction process was divided into 13 load steps. Each load step was described as follows, and the simulation of the construction process is shown in Figure 13.

(1) The emplacement of the lifting tree and the emplacement of the installing cable.

(2) Lifting up to the level 1 m.

(3–12) Each increase of the angle between the branch and the horizontal plane by 5 degrees was one load step, which defines the 3^{rd}–12^{th} load steps.

(13) Lifting to the position was the 13^{th} and final load step.

The comparison of calculated and monitored results of cable force and deformation of key positions is shown in Figures 14–16. As shown in Figure 14, there is fairly consistent agreement on the calculating cable force and the monitored result. The maximum difference of active cable data between calculated results and monitored results was within 4%. The maximum difference of the upper cable data No. 2 between calculated results and monitored results was within 10%. This meant that the calculation model was relatively accurate. The maximum cable force, 860 kN, appeared in the 1^{st} load step of the active cable. The maximum stress of cable was 375.5 MPa. Its design value took into account the influence of vibration, and the safety factor was 5 (0.2 times standard value). So, the maximum stress was 387.3 MPa, which met the design requirements. It could be seen from Figure 15 that the maximum deformation of joint 2 appears in the first load step, and the deformation gradually stabilized with the lifting. The calculated value took each step as an independent state, not considering the gradual process of ascension, so the calculation of the deformation value with ascension was a gradual process. The maximum deformation value of X was 3.6 mm, and the out-of-plane movement was not monitored in the process. The reason was that the out-of-plane disturbance could be eliminated by the double-supported frame. The maximum monitored deformation value of Y was 101.8 mm, and the calculated value was 116.27 mm. The maximum difference was 14.2%. The maximum monitored deformation value of Z was 145.8 mm, and the calculated value was 173.53 mm. The maximum difference was 19%. The No. 2 joint had a large vertical deformation that was also observed in the lifting site. A large vertical deformation occurred at the beginning of the lifting of the support frame connected with the No. 2 joint, as shown in Figure 17, which was further verified in the finite element model. It could be seen from Figure 16 that the maximum deformation of the tower appeared in the first load step, with the lifting and the protection of the cable rope, and the deformation gradually stabilized. The calculated value took each step as an independent state, not considering the gradual process of ascension, so the calculation of the deformation value with ascension was a gradual process. At the same time, the effect of the cable rope was simplified as the out-of-plane (X) displacement, so the difference between calculated results and deformation results was relatively large.

As we know from the above analysis, the calculation model was generally consistent with the actual results. The calculated results of the cable force of the No. 1 upper and lower cables, No. 3 upper and lower cables, and No. 2 lower cable are shown in Figure 18. The deformation calculated results of No. 1 joint and No. 3 joint are shown in Figure 19. As shown in Figure 18, the maximum tensile force of the cable was 379.7 kN, which appears in the No. 1 upper back cable. The cable was within the allowable range of

Table 2: Mechanical properties of stranded wire.

Test items	Technical index	First sample	Second sample	Third sample	Average value
Specified nonproportional extension force $F_{p0.2}$ (kN)	≥318	328.42	327.01	326.51	327.3133
Specified nonproportional extension $R_{p0.2}$ (MPa)	—	1720	1710	1710	1713.333
Maximum force F_m (kN)	≥353	372.13	370.91	367.52	370.1867
Maximum tensile strength F_m (MPa)	1860–2060	1950	1940	1920	1936.667
Maximum total elongation	≥3.5%	7.0%	7.0%	7.0%	7.0%

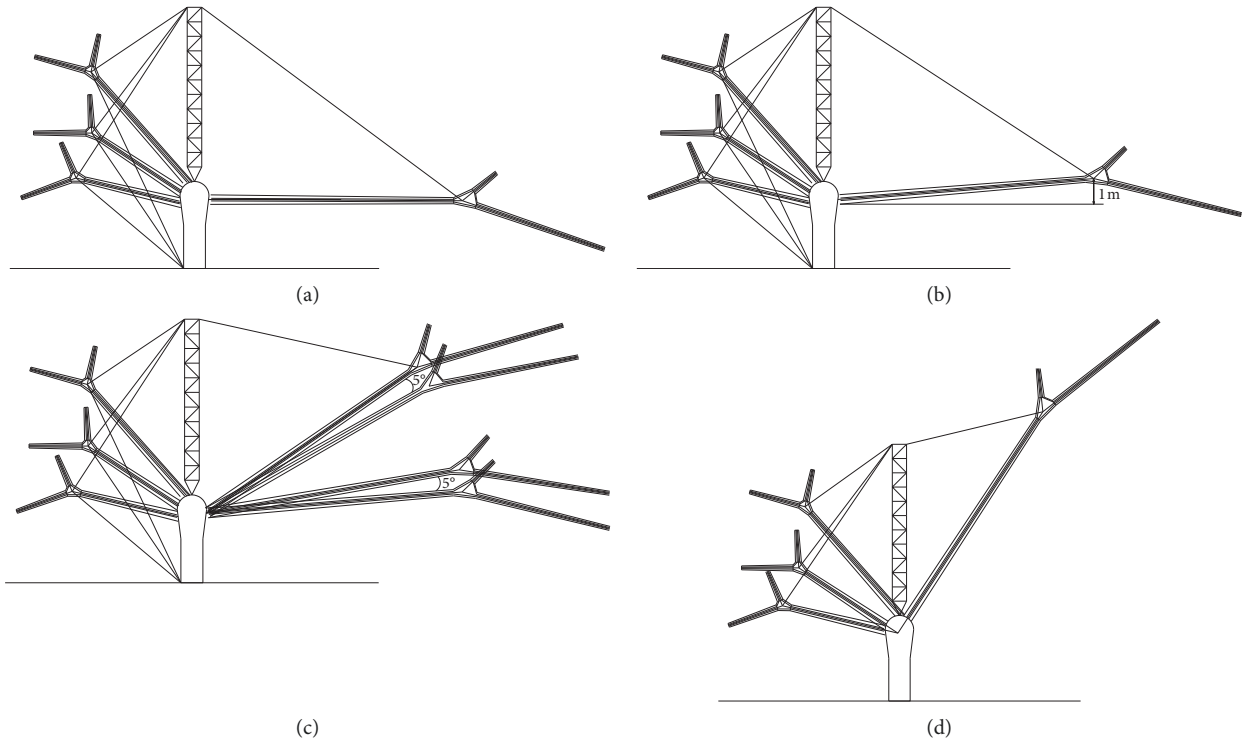

Figure 13: Construction process simulation. (a) Step 1. (b) Step 2. (c) Steps 3–12. (d) Step 13.

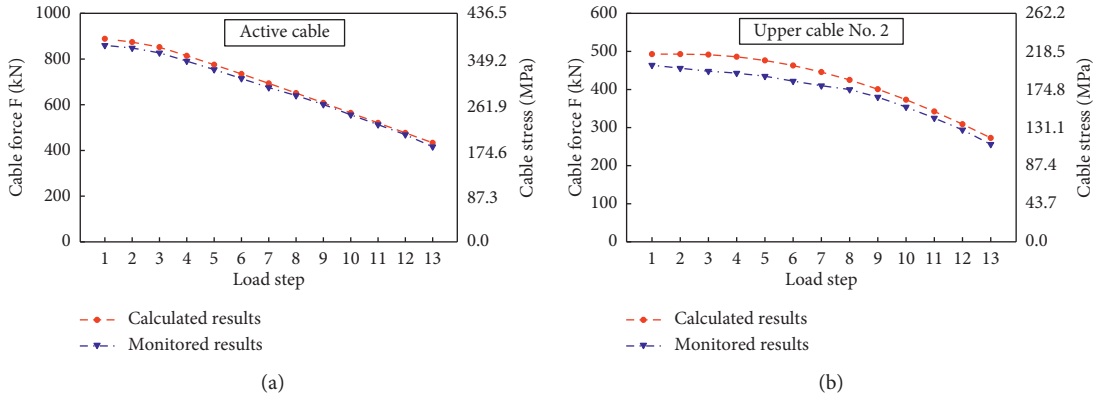

Figure 14: Comparison of calculated and monitored results of cable force. (a) Active cable. (b) Upper cable No. 2.

tension, which indicated that the selection of cable was reasonable. It could be seen from Figure 19 that there was little difference of deformation between No. 1 and No. 3 joints. The reason was that the difference between the cable force corresponding to No. 1 joint and No. 3 joint was small. However, there was no obvious observation of out-of-plane deformation in the site, which indicated that the double scaffold model could solve a out-of-plane

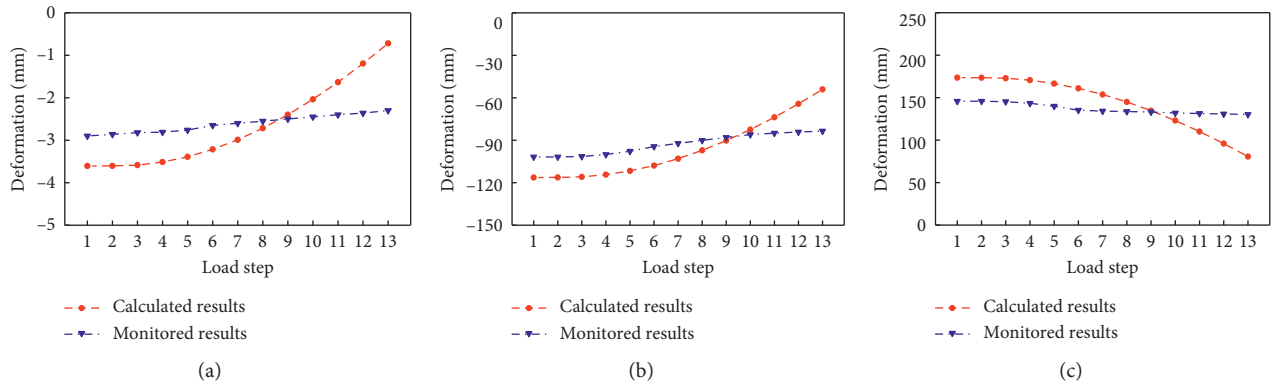

Figure 15: Comparison of calculated and monitored results of deformation of No. 2 joint. (a) X direction. (b) Y direction. (c) Z direction.

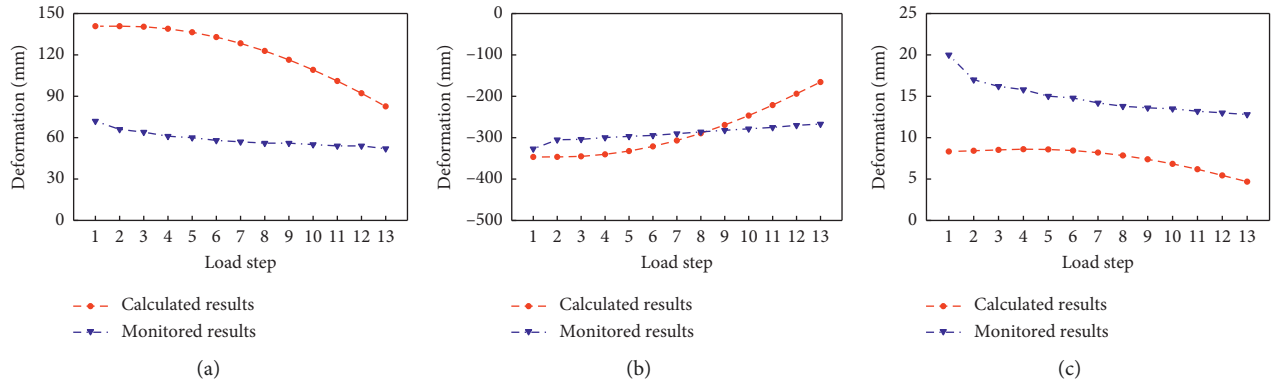

Figure 16: Comparison of calculated and monitored results of top tower deformation. (a) X direction. (b) Y direction. (c) Z direction.

Figure 17: Deformation of scaffold connected to No. 2 joint.

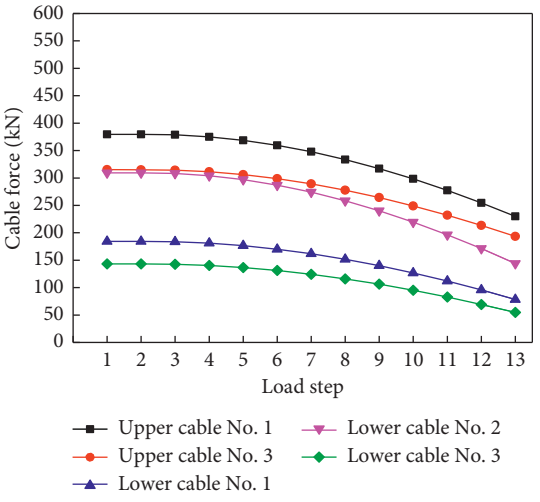

Figure 18: Calculated results of cable force.

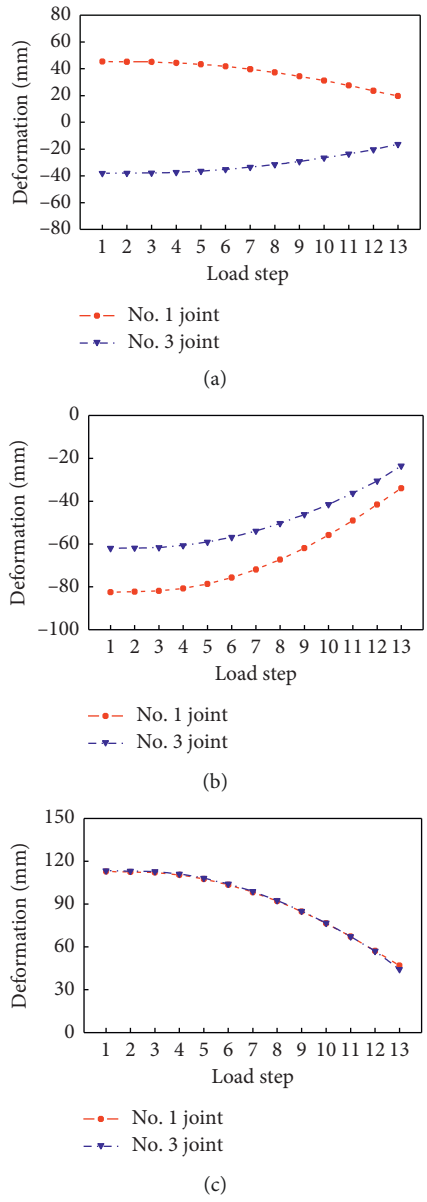

Figure 19: Calculated results of joint deformation. (a) X direction. (b) Y direction. (c) Z direction.

disturbance well. This influence was not considered in the calculation.

6. Conclusion

The construction period of the dendritic column in Niushou Mountain was tight, and the site condition was special. There were many restrictions on the ground and air. The maximum length of the branch was 52 m, and the project, the self-balancing elevating scheme, was introduced. Through the simulation analysis of the construction process and comparison with the monitored results, the following results could be obtained:

(1) A new construction method, self-balancing elevating scheme, was introduced in this paper, which could complete the installation of a large steel structure in a special field safely and efficiently. The improved lifting frame decreased the maximum stress ratio of the lifting chord from 0.98 to 0.657, a reduction of 33%. A new connection joint scheme was proposed to improve the strength and stability of the joint.

(2) A construction monitoring scheme was adopted in this project to ensure construction safety. The maximum cable force and deformation occurred at the beginning of the lifting. Through the simulation of the construction process, the cable force and deformation of key points were obtained. Fairly consistent agreement was found between the simulation results and the monitored results, especially for the force of the active cable and the upper cable No. 2, which indicated that the whole construction process was simulated effectively.

Data Availability

The data used to support the findings of this study are available from the corresponding author upon request.

Conflicts of Interest

The authors declare that they have no conflicts of interest.

Acknowledgments

The research reported herein was supported by research grant no. 16DZ2250600 with funds given by the Shanghai Committee of Science and Technology.

References

[1] C. Xiao, "A study on the construction of space grid structures by the lift-up method," *Spatial Structures*, vol. 1, no. 2, pp. 50–55, 1994.

[2] Z. X. Hou, H. J. Zhang, C. Wang et al., "The constructional techniques of the large span steel structure in the Singapor-eMEGA meeting and exhibition center," *Industrial Construction*, vol. 29, no. 8, pp. 60–63, 1999.

[3] H. Li, F. Zhou, J. Teng et al., "An analysis of monitored and computed strain of the national aquatics center in the states of unloading and daily use," *China Civil Engineering Journal*, vol. 45, no. 3, pp. 1–9, 2008.

[4] F. S. Lu, Q. Q. Wang, G. J. Zhou et al., "Key technology for large-scale grid structure construction of the roof of corridor in Chongqing Jiangbei international airport," *Steel Construction*, vol. 30, no. 198, pp. 81–85, 2015.

[5] V. Meshchersky, "Dynamics of a particle of variable mass," Ph.D. thesis, St Petersburg University of Technology, St Petersburg, Russia, 1897.

[6] R. V. Southwell, *An Introduction to the Theory of Elasticity for Engineers and Physicists*, Oxford University Press, New York, NY, USA, 1941.

[7] V. E. Naumov, "Mechanics of growing deformable solids: a review," *Journal of Engineering Mechanics*, vol. 120, no. 2, pp. 207–220, 1994.

[8] Z. Y. Cao, "Construction mechanics and time-varying mechanics in civil engineering," *China Civil Engineering Journal*, vol. 34, no. 3, pp. 41–46, 2001.

[9] H. Li and J. P. Ou, "Design and implementation of health monitoring systems for cable-stayed bridges (I): design methods," *China Civil Engineering Journal*, vol. 39, no. 4, pp. 39–44, 2006.

[10] G. W. Housner, L. A. Bergman, T. K. Caughey et al., "Structural control: past, present, and future," *Journal of Engineering Mechanics*, vol. 123, no. 9, pp. 897–971, 1997.

[11] T. D. Sloan, J. Kirkpatrick, J. W. Boyd, and A. Thompson, "Monitoring the in-service behaviour of the Foyle bridge," *Structural Engineer*, vol. 70, no. 7, 1992.

[12] Q. S. Li, J. R. Wu, S. G. Liang, Y. Q. Xiao, and C. K. Wong, "Full-scale measurements and numerical evaluation of wind-induced vibration of a 63-story reinforced concrete tall building," *Engineering Structures*, vol. 26, no. 12, pp. 1779–1794, 2004.

[13] J.-Z. Su, Y. Xia, L. Chen et al., "Long-term structural performance monitoring system for the Shanghai Tower," *Journal of Civil Structural Health Monitoring*, vol. 3, no. 1, pp. 49–61, 2013.

[14] X. Cui, Y. Guo, and K. Ye, "Research on the construction mechanic method of long-span steel structures," *Engineering Mechanics*, vol. 23, no. 5, pp. 83–88, 2006.

[15] H. Lin, J. Wu, H. Chen, Z. Yang, and Q. L. Zhang, "Study on rotate lifting method in large imbalanced weight branching structure," *Construction Technology*, vol. 44, no. 18, pp. 117–122, 2015.